PK/PD modelling of combed-shaped PEGylated salmon calcitonin conjugates of differing molecular weights

Sinéad M. Ryan [a,b], Jesús M. Frías [b], Xuexuan Wang [a], Claire T. Sayers [c], David M. Haddleton, [c] and David J. Brayden [a,*]

[a] UCD School of Veterinary Medicine and UCD Conway Institute, University College Dublin, Belfield, Dublin 4, Ireland; [b] School of Food Science and Environmental Health, Dublin Institute of Technology, Cathal Brugha Street, Dublin 1, Ireland; [c] Department of Chemistry, University of Warwick, Coventry CV4 7AL, UK.

* Corresponding author. Tel.: +353 1 7166013; fax: +353 1 7166019.
E-mail address: david.brayden@ucd.ie

Abstract

Salmon calcitonin (sCT) was conjugated via cysteine-1 to novel combed-shaped end-functionalised poly(PEG) methyl ether methacrylate) (sCT-P) comb-shaped polymers, to yield conjugates of total molecular weights (MW) inclusive of sCT: 6.5, 9.5, 23 and 40 kDa. The conjugates were characterised by HPLC and their *in vitro* and *in vivo* bioactivity was measured by cAMP assay on human T47D cells and following intravenous (i.v.) injection to rats, respectively. Stability against endopeptidases, rat serum and liver homogenates was assessed. There were linear and exponential relationships between conjugate MW with potency and efficacy respectively, however the largest MW conjugate still retained 70% of E_{max} and an EC_{50} of 3.7 nM. *In vivo*, while free sCT and the conjugates reduced serum [calcium] to a maximum of 15-30 % over 240 min, the half life (T½) was increased and the area under the curve (AUC) was extended in proportion to conjugate MW. Likewise, the polymer conferred protection on sCT against attack by trypsin, chymotrypsin, elastase, rat serum and liver homogenates, with the best protection afforded by sCT-P (40 kDa). Mathematical modelling accurately predicted the MW relationships to *in vitro* efficacy, potency, *in vivo* PK and enzymatic stability. With a significant increase in T½ for sCT, the 40 kDa MW comb-shaped PEG conjugate of sCT may have potential as a long-acting injectable formulation.

Keywords: salmon calcitonin, PEGylation, conjugated peptides, osteoporosis, pharmacokinetic modelling, comb-shaped polymers

1. Introduction

Inadequate delivery is a barrier to the effective administration of many promising biotech molecules [1]. Parenterally-administered proteins and peptides tend to be rapidly cleared from circulation by the reticuloendothelial system (RES) or metabolised by serum and liver peptidases leading to loss of biological activity. Oral delivery is even more problematic than the parenteral route, as peptide and protein-based molecules are metabolised by serine proteases, degraded at varying intestinal pH values, and have poor small intestinal epithelial permeability (i.e. typical Class III agents in the Biopharmaceutical Classification System) [2]. A number of strategies have been devised to improve the pharmacokinetics (PK) for parenterally-administered proteins. One of the

most successful commercial approaches has been the covalent attachment of poly(ethylene glycol), i.e. PEGylation [3,4]. Improved PK is largely attributed to the increased molecular size conferred by PEG on the conjugate, thereby masking the protein surface from proteolytic attack, decreased recognition by phagocytes of the RES, and reduced glomerular filtration [5]. Examples of marketed long-acting injected PEGylated biopharmaceuticals are the anti-VEGF aptamer, Pegaptanib (Macugen®, OSI Pharmaceuticals, USA), for treatment of wet macular degeneration, and Pegfilgrastim (Neulasta®, Amgen Ltd, USA), granulocyte-stimulating colony factor (G-CSF) for treatment of chemotherapy-induced neutropenia.

In this study, sCT was used to further examine a novel type of comb-shaped PEGylation. sCT (molecular weight (MW) 3432 Da) is a more potent analogue of human CT, a small 32 amino acid peptide [6]. The primary structure is characterised by a disulfide bridge between two cysteine (cys) residues at positions 1 and 7 and a proline amide moiety at the C terminus; it also displays an α-helix and β-sheet, but has no tertiary structure. In bone, sCT acts primarily by inhibiting osteoclast cell-mediated bone resorption, although it may have an anabolic effect on chrondrocytes [7]. It is licenced to treat hypercalcaemia, Paget's disease and as a second-line treatment for post-menopausal osteoporosis. Although its analgesic effects are well known, there is renewed commercial interest in the peptide due to its potential benefit in osteoarthritis [8]. It is administered by subcutaneous or intra-muscular injections, or more commonly via the nasal route [9]. Due to its short terminal half-life (T½) following parenteral administration, regular injections are required and patient compliance is low. Although preferable to nasal, successful oral formulations of sCT have been elusive [10]. Longer-acting injections of sCT would have an obvious advantage over current injected formulations.

We recently demonstrated specific cysteine-1 conjugation of sCT to a combed-shaped end-functionalised poly(PEG- methyl ether methacrylate) comb-shaped polymer, (sCT-P) [11]. The 6.5 kDa MW conjugate had increased proteolytic stability compared to both free sCT and a linear PEG version of similar total MW. In addition to lengthening the half-life of sCT following injection to rats, *in vitro* and *in vivo* efficacy and potency was retained by the conjugate [11]. The aim of the present study was to evaluate the effects of increasing the MW of the comb-shaped polymer conjugated onto sCT on both *in vitro* bioactivity and *in vivo* PK following i.v. injection to rats. Whilst increased polymer MW generally improves peptide stability and lengthens the T½, it may interfere with biological functions at the receptor level due to steric hindran2e [13]. Therefore, an appropriate polymer MW should be selected to balance pharmacodynamics (PD) and PK. We synthesised a range of sCT-P conjugates of different MW attached to the methacrylate group via cys-1 and investigated *in vitro* biological activity, stability and cytotoxicity. A two compartment model was used to model free sCT kinetics and a first order process modelled release of free sCT from the conjugates. We then compared the release rate constants (k_{rel}) between polymers and ascertained the effects of MW.

2. Materials and Methods

2.1. *Materials*

sCT was purchased from PolyPeptide Laboratories (Denmark). The Parameter™ cAMP (EIA) kit was obtained from R&D systems, UK, and the sCT (EIA) kit was

purchased from Bachem (UK). $Na(CN)BH_3$ was supplied by Sigma Aldrich, UK. Tissue culture reagents were obtained from BioSciences, Ireland.

2.2. *Synthesis of sCT- poly(poly(ethylene glycol) methyl ether methacrylate) (sCT-P) conjugates*

Poly(poly(ethylene glycol) methyl ether methacrylate) polymers of differing MW were prepared by Transition Metal-Mediated Living Radical Polymerization (TMM-LRP) [13, 14]. Each polymer (P) was conjugated to the *N*-terminal cys-1 at of sCT by reductive amination [15]. To make sCT-P (6.5 kDa), a solution of sCT (100 mg, 0.029 mM) in 100mM acetate buffer pH 5.0 (30 mL) was added to a solution of 6.5 kDa aldehyde-functionalised poly(poly(ethylene glycol) methyl ether methacrylate) (1.91 g, 0.29nM), previously dissolved in 30 mL of the same buffer. Aqueous 25 mM $NaCNBH_3$ (3.0 mL, 0.075mM) was then added and the resulting solution was left stirring at ambient temperature and monitored by RP-HPLC, taking 150 µL aliquots of the reaction mixture and dilute them in 1.35 mL of mobile phase A (90 % HPLC grade water, 10 % MeCN and 0.05 % tri-fluoroacetic acid (TFA)) prior to analysis. The final conjugates were purified by cationic ion-exchange fast protein liquid chromatography (IE-FPLC) using a gradient of NaCl in 20 mM aqueous sodium acetate (pH 4.0). The MW of the sCT-P conjugates were: 6.5, 9.5, 23 and 40 kDa, each inclusive of sCT (3.4 kDa).

2.3. *Reverse Phase HPLC analysis*

Characterisation of sCT-P conjugates was monitored by reverse phase (RP) HPLC. Samples were analysed with a Varian 920 HPLC using a Luna 5µ C18(2) column 250 × 4.6 mm (Phenomenex, UK). Gradient elution was carried out at a flow rate of 1.0 mL/min, with a mobile phase A containing: 99.9% H_20 and 0.1% TFA, and a mobile phase B, containing: 99.9% acetonitrile and 0.1% TFA. The gradient sequence was: 20-35% B from 0-10 min, 35-37% B from 10-20 min and 37-20% B from 20-25 min. Samples were monitored at a UV absorbance of 215 nm and 280 nm.

2.4. *MW analysis of sCT-P conjugates*

The sCT-P (6.5 kDa) conjugate was analysed by matrix assisted laser desorption ionisation-time of flight mass spectrometry (MALDI-TOF MS, Bruker UltraFlex III MALDI-TOF mass spectrometer) and size-exclusion chromatography (SEC)-HPLC. SEC-HPLC was carried out on the other conjugates (9.5, 23, 40 kDa) using a BioSep-SEC-S-2000 and S-3000 columns 300 × 7.8 mm (Phenomenex, UK). Samples were eluted with 50 mM PO_4 pH 6.8 at a flow rate of 1 mL/min, and monitored at a UV absorbance of 215 nm and 280 nm. MALDI-TOF MS was not suitable for these larger MW samples. The integrity and purity of the derivatives were monitored using RP-HPLC (Section 2.3).

2.5. Identification of the PEGylation site of sCT on PolyPEG® derivatives

Identification of the attachment site of poly(poly(ethylene glycol) methyl ether methacrylate) to cys-1 of sCT was confirmed by selective tryptic digestion [16]. Briefly, 50-200 µM of sCT-P was digested using trypsin (0.5 µM) in ammonium bicarbonate buffer (0.05 M) incubated at 37°C for a minimum of 12 hr. The reaction was stopped by

addition of 5 % acetic acid. The trypsin-digested samples were analysed using RP-HPLC and MALDI-TOF MS.

2.6. ***In vitro bioactivity: intracellular cAMP stimulation in human T47D cells***

The capacity of sCT-P conjugates to increase intracellular cAMP was assessed [17]. T47D human breast cancer cells expressing CT receptors were maintained in RPMI-1640 medium containing 1 % penicillin–streptomycin, 10 % fetal bovine serum, and insulin (0.2 IU/mL). Cells were seeded on 24 well plates at an initial density of 1.0×10^6 cells/well and incubated in 95% O_2:5% CO_2 at 37 °C for 24 hr. Media was replaced with serum-free media and incubated for a further 24 hr. After washing with HBSS, cells were pre-incubated with the serum free medium supplemented with the phosphodiesterase inhibitor 3-isobutyl-1-methyl-xanthine (IBMX, 0.2mM) at 37 °C for 30 min. The cells were incubated with sCT-P conjugates for 15 min. The adenylate cyclase activator, forskolin (10 μM), was used as a positive control. After removing the media, intracellular cAMP was extracted from cells and measured by ELISA. Results were analysed using R Statistical Language [18] and represented as an E-max model.

2.7. Stability studies: intestinal enzyme metabolism

sCT-P conjugates were incubated with intestinal enzymes in sodium acetate (50 mM) buffer at a pH 4.5. It also contained TPCK (N-p-tosyl-Lphenylalanine chloromethyl ketone)-treated trypsin (0.5 μM), TLCK (1-chloro-3-tosylamido-7-amino-2-heptanone)-treated chymotrypsin (0.1 μM) and elastase (0.48 μM). Enzymes and substrates were incubated separately at 37 °C for 15 min, before co-incubation. Samples were withdrawn at 0, 1, 5, 10, 15, 20, 30 and 60 min. All samples were analyzed for the capacity to induce cAMP in T47D cells, previously shown to match the structural stability by RP-HPLC analysis [11]. Rate constants and half lives for sCT-P conjugates were calculated by assuming first order kinetics.

2.8. ***Stability studies: rat liver homogenates and serum***

A fresh liver harvested from a sacrificed Wistar female rat (240 g) was soaked in ice cold saline and homogenized in 10mM PBS at pH 7.4. The mixture was centrifuged at 2000 rpm at 4°C for 2 min, and the supernatant collected. Rat serum was collected by centrifugation (8500 rpm, 15 min) at 4°C. Protein concentrations were measured and adjusted to the final bovine serum albumen equivalent concentration of 20 mg in 10mM PBS (pH 7.4). After 15 min equilibration at 37°C, liver homogenates or serum were then co-incubated with sCT-P conjugates. Samples were taken at 0, 1, 5, 10, 15, 20, 30 and 60 min and all samples were analysed for bioactivity on T47D cells.

2.9. ***Lactate dehydrogenase (LDH) release from Caco-2 monolayers***

Caco-2 cells were cultured as filter-grown monolayers according to previous methods [19]. sCT and sCT-P conjugates were added to the apical side of monolayers at a concentration of 10 μM. Medium and SDS (0.1 %) were used negative and positive controls respectively. Samples were taken from the apical side at different time points for 120 min and assayed for LDH release using an ELISA microplate reader (Tecan SpectraFlour Plus®). The absorbance was measured at 450 nm, with the reference absorbance at 620 nm. Cell viability was expressed as the percentage of absorbance of

test compounds compared with that of cells incubated with media alone. Transepithelial electrical resistance was measured using an EndOhm® electrode system (World Precision Instruments, UK) across confluent monolayers [19].

2.10. ***Hypocalcaemia and PK of sCT-P conjugates in rats***

7-8 week-old male Wistar rats (200-300g) were anaesthetized using intra-peritoneal injections of ketamine (75 mg/kg) and xylazine (10mg/kg). Rats were injected *via* the tail vein at a dose of 40µg/kg (i.e. 200 IU/mL/kg) sCT for each formulation in triplicate unless stated. 0.2mL blood samples were obtained via cardiac puncture using a 26G needle fitted with a 1mL heparinised syringe before administration and then typically at 15, 30, 60, 120, 180, 240, 360 and 480 min after injection. Serum samples were analysed for calcium using a Randox Laboratory clinical chemistry colorimetric analyser [11]. sCT concentrations in serum were detected by using an EIA kit (Bachem, UK), with a limit of detection of 0.02-25 ng/mg. PK parameters including AUC and terminal T½ were calculated using WinNonLin® 5.2 software (Pharsight Corp., USA). All animal experimental procedures in the study adhered to the Principles of the Laboratory Animal Care (NIH Publication# 85–23, revised in 1985) and were performed in compliance with the Irish Department of Health and Children animal licence number, B100/3709, following approval by the UCD Animal Research Ethics Sub-committee.

2.11. ***Two compartmental model analysis of sCT in vivo data***

A two compartmental model considering serum (central) and peripheral pools (Fig. 1A) was used to describe the PK of serum sCT following i.v. injection to rats [20, 21]. Considering first order for sCT movement, the resulting system of ordinary differential equations (ODE) defining the Model I were:

$$dy_1/dt = -k_{12}\, y_1 + k_{21}\, y_2 - k_{deg}\, y_1 \quad \text{(Eq.1)}$$
$$dy_2/dt = k_{12}\, y_1 - k_{21}\, y_2 \quad \text{(Eq. 2)}$$

Where k_{12} and k_{21} are the first rate transfer constants between compartment 1 and 2 and vice versa, and k_{deg} is the first order degradation constant of sCT in serum [21]. To these parameters, sCT_0, the initial concentration in the central compartment (y_1 at t=0), was added to accommodate for intra-subject variation. The initial concentration of sCT in the inner compartment was assumed to be zero. Non-linear least squares regression was performed using the *nlme*ODE library [22, 23], together with the *gnls* function from the *nlme* library [24] of R Statistical Language [18]. The *nlme* ODE library uses the ODEPACK Fortran library for the solution of ordinary differential equation systems arising from the PK models [25]. The *gnls* function employs a Gauss-Newton method to solve the nonlinear least squares optimization problem. No weights and a Gaussian error function were used to estimate the primary parameters k_{12}, k_{21}, k_{deg} and sCT_0 (sCT in central compartment at time of i.v. injection) from the free sCT PK data. In order to ensure non-negative estimates while keeping the optimization problem unconstrained, the natural logarithm transformation of the parameters was estimated. Results are presented as the antilog transformation of the estimates and the associated standard error propagated [20].

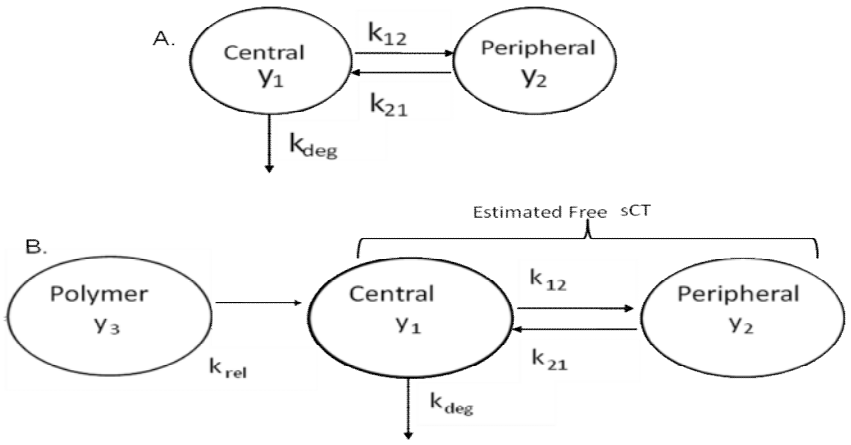


Fig. 1. Two compartmental models describing PK of sCT in rat serum following i.v. administration. **A**. sCT, **B**. sCT-P conjugates.

2.12. Two compartmental model analysis of sCT-polymer derivatives in vivo data

To further model the PK of the sCT-P conjugates, a first order release process of sCT from the conjugates to release free sCT to the central compartment was added to Model I to yield Model II (Fig. 1B). Assuming first order for transfers, the system of ODE defining Model II is:

$$dy_1/dt = -k_{12}\, y_1 + k_{21}\, y_2 - k_{deg}\, y_1 + k_{rel}\, y_3 \quad \text{(Eq. 3)}$$

$$dy_2/dt = k_{12}\, y_1 - k_{21}\, y_2 \quad \text{(Eq. 4)}$$

$$dy_3/dt = -k_{rel}\, y_3 \quad \text{(Eq. 5)}$$

Where k_{12} and k_{21} are the first rate transfer constants between compartment 1 and 2 and vice versa, k_{deg} is the first order degradation constant of free sCT in serum as described in Model I, and k_{rel} is the first order release constant of sCT from the polymer. To these unknown parameters, $y_{3,0}$, the concentration of conjugated sCT after i.v. injection to the polymer compartment 3 (y_3 at t=0) was estimated with a random effect to allow for variations in dose levels between subjects. While k_{rel} may vary between different polymers, the rest of the parameters ($y_{3,0}$, k_{12}, k_{21} and k_{deg}) in the model are likely to be shared by free sCT and sCT-P. The estimated parameters from Model I were used in Model II to describe the PK of those conjugates, while k_{rel} and y_3 was estimated for each conjugated polymer in order to compare the release constants (k_{rel}). The non-linear mixed effect models were fitted by use of the *nlme*ODE and the *nlme* functions, which used the approximation from Lindstrom *et al*. [26] to fit the non-linear mixed effects model. Both the error term and the between-subject random effect added to the release constant k_{rel} followed independent normal distributions. Non-linear mixed effect models were fitted with the data from each individual sCT-P conjugate. This served to test the significance of the release constant parameter k_{rel}. Using the resulting individual estimates (k_{rel}), a dependence between the natural log release constant and the MW of the conjugated polymer was proposed to model all data simultaneously. A likelihood ratio test with a model without such dependence was used to test for significance of the dependence of the release constant rate on the MW of sCT-P conjugates.

2.13. Statistical analysis

Tukey-HSD post hoc ANOVA comparison and generation of confidence intervals was performed using R Statistical Language [18]. $P < 0.05$ was the required level to denote statistical significance.

3. Results

3.1. Characterization of sCT-P conjugates

Chemical structure, preparation, purification and characterisation of the sCT-conjugated polymers has been previously published, including ion-exchange (IE), reverse-phase HPLC and MALDI-TOF [27, 28]. SEC-HPLC analysis confirmed high purity and predicted the molecular weights of all sCT-P comb-shaped conjugates (Table S1). Conjugation reactions were monitored over time by RP-HPLC where the profile showed a reciprocal relationship between the sCT peak gradually disappearing at an approximate elution volume of 17.0 mL and the conjugate peak gradually appearing over the same period at an approximate elution volume of 20 mL. Fig.S1 shows the data for sCT-P (9.5 kDa). sCT-P conjugates were further purified by IE-FPLC, an example shown for the 6.5 kDa conjugate (Fig.S2). Fractions obtained from (IE)-FPLC were then analysed by SEC-HPLC to evaluate purity (Fig.S3). Identification of the attachment site was achieved by analogy as previously described [12]. The conjugation site of the purified conjugates at cysteine-1was determined and confirmed by tryptic digestion followed by RP-HPLC and MALDI-TOF MS analysis of the digested fragments (data not shown, but see [12] for data on the sCT-P (6.5 kDa) conjugate).

Free sCT and sCT-P conjugates elevated intracellular cAMP in a concentration-dependent manner (Fig. 2a). The EC_{50} and E_{max} values (Table 1) determined for each conjugate were inserted into a global fit model. From it, an exponential relationship was obtained for the former (Fig. 2b) and a linear relationship was obtained for the latter with respect to MW (Fig. 2c). In sum, the higher the MW of polymer attached to sCT, the higher the potency and the lower the efficacy. However, even for the largest MW (sCT-P (40 kDa) conjugate, 72 % of E_{max} was still retained compared to free sCT and the potency was within 1-2 log concentrations.

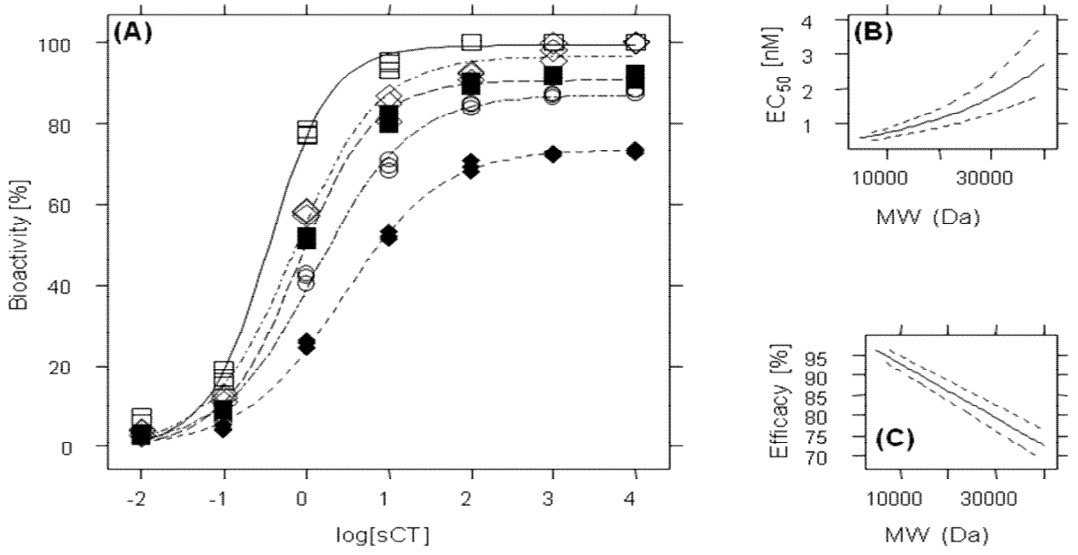


Fig. 2. Modelling of bioactivity dependence on MW. A. Concentration-response curves of sCT and P conjugates. Continuous lines show prediction of the three parameter concentration-response curve fit with Hill slope=1. Free sCT □, sCT-P (6.5kDa) ◊, sCT-P (9.5kDa) ■, sCT-P (23kDa) ○, sCT-P (40kDa) ♦. B. Dependence of EC_{50} on MW. C. Dependence of efficacy on MW. Discontinuous lines show 95% confidence limits of predictions.

3.3. Stability of sCT-P conjugates: intestinal enzymes, liver homogenates and serum

The stability of sCT conjugates against exposure to intestinal enzymes was analysed by cAMP responses generated in T47D cells. sCT was rapidly degraded by trypsin, chymotrypsin, elastase and in combination. sCT-P conjugates displayed significantly increased resistance to the individual intestinal enzymes and in combination, and the higher the MW, the greater the protection (Fig. 3). The largest conjugate sCT-P (40 kDa) gave excellent protection to sCT when incubat C r 60 min with the three individual enzymes alone and in combination. The degradation half life of sCT-P (40 kDa) was 11 times longer than that of sCT-P (6.5 kDa) ($p<0.005$), when all three proteolytic enzymes were present. An almost identical pattern was also observed for the conjugates in rat liver homogenates and serum.

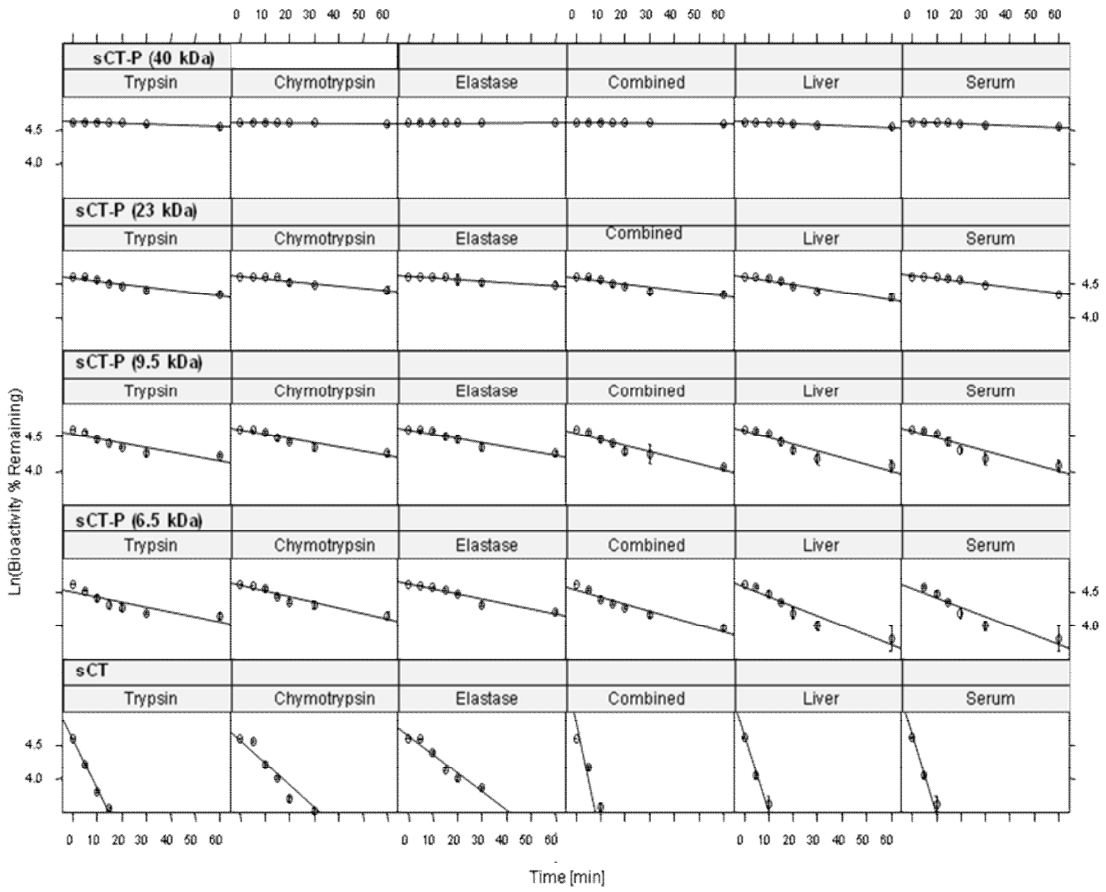


Fig.3. Degradation profiles of conjugates incubated with enzymes, liver and serum.

A comparison of the apparent first order reaction rate constants of each conjugate in the presence of serine proteases, rat blood serum and rat liver homogenate as determined by cAMP measurements revealed that there was dependence of reaction rate constant (k) of sCT with polymer MW (Fig. 3). As the MW of the conjugate increased, the degradation rate of sCT decreased.

3.4. Cytotoxicity evaluations on Caco-2 monolayers by LDH

sCT conjugates at a concentration of 10 µM showed relatively low levels of cytotoxicity following 120 min exposure (Fig.S.4). Cytotoxicity increased as the MW of conjugate was increased. For sCT-P (6.5 kDa), 10% of cells were unviable, whereas for sCT-P (40 kDa), 28% were unviable. Similar to the pattern observed for LDH release, the TEER decreased as the MW of the conjugates increased. A maximum and reversible TEER decrease of 28% was also observed for sCT-P (40 kDa) compared to Caco-2 exposed to media alone after 120 min (data not shown).

3.5. *In vivo* hypocalcaemia and PK of sCT-P conjugates in rats

sCT and sCT-P conjugates were assessed for their capacity to induce a hypocalcaemic response in rats following i.v. injection. At equivalent doses of 200 IU/kg sCT, sCT–P conjugates significantly reduced serum [calcium] over the test period. Compared to free sCT and to each other, the calcium profiles after i.v. injections of sCT conjugates did not however, show any statistical differences (Table 1). The range of serum [calcium] reduction was 15-30%, and 30% is typically the maximum reduction detectable by the assay [11].

Using the same blood samples, serum [sCT] were also determined by ELISA following i.v. administration of sCT and sCT-P conjugates. Free [sCT] was rapidly eliminated. In contrast, sCT-P conjugates had much longer T½ values (Table 1). The values for sCT-P (6.5 kDa) and sCT-P (23 kDa) were not different due to high inter-animal variations, but their $AUC_{0\text{-}480\ min}$ values were higher than free sCT ($P < 0.0001$, $P < 0.05$, respectively). Following administration of sCT-P (6.5, 9 and 40 kDa), plasma [sCT] was relatively constant, suggesting a sustained release of sCT (Fig. 4). Importantly, there was a significantly longer T½ and larger AUC at 8 hours for sCT-P (40 kDa) compared to sCT itself and the other sCT-containing conjugates.

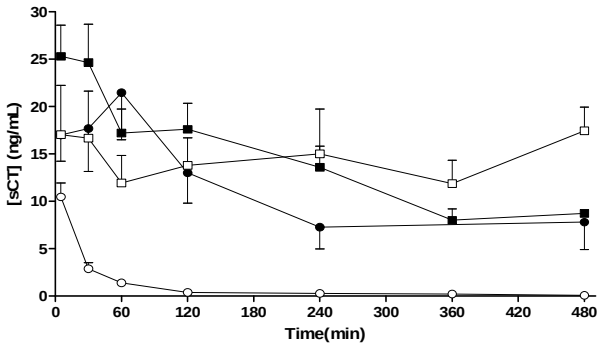


Fig.4. sCT levels in rat serum after i.v. administration of sCT (O), sCT-P (6.5 kDa) (■), sCT-P (23 kDa) (●), and sCT-P (40 kDa) (□). Serum samples at time zero in which no sCT was detected were used as background. Mean +/- SEM of 3-15 determinations.

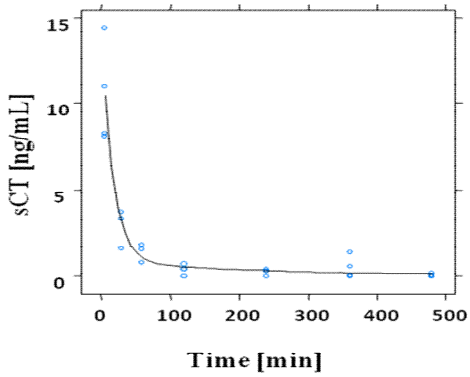
Table 1.
Comparison of *in vitro* efficacy and *in vivo* PK and PD of sCT and sCT-P conjugates in rats.

	cAMP in T47D EC_{50} (nM)	Maximum % hypocalcaemia (i.v.)	$T_{1/2}$ (min) for sCT in serum	$AUC_{0\text{-}480nm}$ (ng.min/mL) sCT in serum
sCT	0.7 (0.2)	23.5 (1.3)	41.8 (12.4)	435 (56)
sCT-P (6.5 kDa)	1.0 (0.1)	14.7 (4.9)	631.9 (341.9)	4594 (519) ***
sCT-P (9.5 kDa)	1.2 (0.1)	ND	ND	ND
sCT-P (23 kDa)	2.5 (0.1)	27.1 (6.2)	668.3 (374.7)	3770 (856) *
sCT-P (40 kDa)	3.7 (0.2)	30.0 (6.5)	1425.6 (257.0) **	6459 (1435) *

Mean(SEM) of 3-12 determinations. ND, not determined. * p<0.05, ** p<0.01. *** p<0.001. compared to sCT.

3.6. PK modelling of sCT following i.v. administration to rats

The serum concentration of sCT and sCT-P conjugates after i.v. administration was fitted using Model I (free sCT) and Model II (sCT-P conjugates). Model I (Fig.1A) predicted the distribution of [sCT] adequately (Fig.5). Non-linear regression was used to calculate the kinetic parameters, k_{12}, k_{21} and k_{deg}. The estimated model parameters had an associated error of the order of 10%, which was considered a reasonable precision to predict the fate of free sCT in plasma. The PK parameters estimated using Model I and free sCT were then used in Model II to predict the PK of sCT-P after i.v. injection.



Parameter	Estimate	SEM
k_{12}	0.028 min^{-1}	0.008
k_{21}	0.008 min^{-1}	0.005
k_{deg}	0.026 min^{-1}	0.007
sCT_0	10.44 ng/mL	0.10
σ	0.2 ng/mL	

Fig.5. Analysis of free sCT data following i.v administration to rats using a two compartmental model to estimate parameters, k_{12},k_{21}, k_{deg} and sCT_0.

Estimates of the release constant (k_{rel}) and the equivalent initial serum [sCT] after injection ($y_{3,0}$) of each individual sCT-P conjugate were built using non-linear mixed

effect modelling. On top of those two fixed parameters, and in order to account for the high inter-subject variability observed, a random effect allowing for inter-subject variation in the initial concentration of sCT-P was made. While ($y_{3,0}$) and its corresponding random effect are nuisance parameters, k_{rel} provided the generation rate of sCT from sCT-P conjugates. As the conjugated polymer increased in MW, k_{rel} decreased (Fig.6), providing a longer release period for sCT, in agreement with the data obtained (Fig 4). By fitting the data of all polymers to a single model containing a dependence of the $\ln(k_{rel})$ with polymer MW, an intercept of -5.4±0.3 $\ln(min^{-1})$ and a slope of -0.053±0.016 $\ln(min^{-1})$ / kD were estimated.

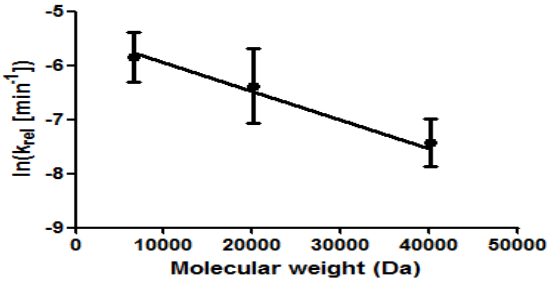


Fig.6. Influence of polymer MW on release rate constant of sCT.

4. Discussion

Several efficacious and safe PEGylated products have been on the market for over 15 years, and ten PEGylated products have been approved to date [29]. Although PEG is an approved biocompatible polymer, individual components of the methacrylate-based PEG, (poly(poly(ethylene glycol) methyl ether methacrylate) are not. Important components include the methacrylic backbone and the terminal aldehyde, previously shown to induce low cytotoxicity to Caco-2 and mucous-covered HT29-MTX-E12 intestinal monolayers [11]. While increasing MW of the polymer seemed to increase cytotoxicity in Caco- 2, levels were still low. Studies will need to be carried out to examine the fate of poly(poly(ethylene glycol) methyl ether methacrylate) and its metabolites in body compartments and tissues as there is potential for accumulation. This is especially relevant in the current example where the polymer is the major component of the conjugate compared to the peptide, and where repeated dosing will be necessary. The kidney clearance threshold of protein is estimated at 60 kDa [4]. Assuming that polymer hydrodynamic volume will almost double the effective molecular diameter, similar to branched PEGs [30], sCT-P (40 kDa) will therefore be too large for kidney filtration if it is not metabolized into smaller components. In theory, the PEG teeth should break away from the methacrylate backbone due to esterase action, thereby permitting renal filtration and this is the basis of ongoing study. It is notable that while PEG itself has Generally Regarded As Safe (GRAS) status as a “non-active” excipient, there are historical reports that it can induce epithelial vacuolisation in rat renal cortical tubules following chronic repeated parenteral administration of high doses of large MW PEGs [31]. An initial toxicology study carried out in rats using a commercially available form of the comb-shaped polymer (PolyPEG®, Warwick Effect Polymers, UK), did not find any evidence of vacuolisation in renal epithelia following repeated dosing of up to

200mg to rats [32]. While undesirable, there is little evidence to date that vacuolisation has any deleterious effects on renal function.

The main drawback associated with peptide and protein PEGylation is the potential for reduced biological activity, however, this can be compensated by a longer elimination T½ and reduced clearance. A well-cited example is PEGylated interferon α-2a (Pegasys®, Roche, USA). The 40 kDa branched PEG conjugate retained only 7% of the antiviral activity of the native protein, but still displayed improved PK following weekly injections *in vivo* in hepatitis C patients [33]. In contrast, bioactivity analysis from the T47D cAMP assay indicated that the potency and efficacy of sCT-P of increasing MW compared well to native sCT, with sCT-P (40 kDa) retaining 72% of the maximum bioactivity. From the global fit model, a linear and indirect relationship was established between efficacy and conjugate MW and there was an exponential and direct dependence on EC_{50} with conjugate MW. It appears therefore that access to the CT receptor has not been impeded by conjugation to cysteine-1 and there is no evidence that sCT simply dissociates from the polymer in solution [11].

sCT has multiple peptidase cleavage sites and is therefore susceptible to proteolytic degradation in the small intestine. To reduce metabolism, a linear lys-18-PEG_{2K}-sCT displayed enzymatic stability, reduced systemic clearance and enhanced hypocalcaemia following intra-duodenal administration to rats [34]. Another sCT-mPEG conjugate with mono- and di- mixtures also had reduced clearance and an extended $T_{1/2}$ compared to unmodified sCT [35]. For the sCT-Lys_{18}-PEG conjugates, increased proteolytic stability and an extended $T_{1/2}$ are clearly associated with increased PEG MW [36]. sCT-P (6.5 kDa) conjugated to cys-1 was more stable than native sCT and, more importantly, than sCT conjugated to linear sCT-PEG (5 kDa) [11]. All conjugates showed substantial resistance to the trypsin, chymotrypsin and elastase alone and in combination, as well as following exposure to rat serum and liver homogenates. Improved stability was observed as the MW of the conjugate increased, with sCT-P (40 kDa) providing almost total protection. In our assessment of stability, we used *in vitro* bioactivity analysis as a PD surrogate, since we previously showed a very close correlation between the cAMP assay and HPLC analysis.

Serum [calcium] and [sCT] following i.v. administration of sCT were measured. Free sCT and the sCT conjugates induced similar hypocalcaemia and the reductions obtained were typical of the maximum achieved following i.v. administration [37]. The non-linear relationship between serum calcium reduction and [sCT] suggests a highly complex relationship [21, 38], and there is obvious difficulty in rank-ordering formulations when the window of the calcium reduction is so narrow. Thus, measurement of serum [sCT] is the more sensitive screening assay. Still, all sCT conjugates were bioactive *in vivo*, thus confirming the *in vitro* bioassay data. Serum [sCT] decreased rapidly following i.v. administration of free sCT and levels were below the detection limit after 120 min. The conjugates were, however, detectable up to 8 hr following administration and sCT-P (40 kDa) yielded a T½ over 30 times longer than sCT. For interferon-α 2a, plasma concentrations did not peak until 23-26 hr following i.v. administration of a PEGylated conjugate of similar MW [39] to the sCT-P (40 kDa) conjugate.

Recently, models of the PK/PD relationship for sCT have described the interactions between osteoclasts and osteoblasts [40]. Compartmental models have been

previously used to describe the kinetics of sCT [21], and the present work confirms that the PK of free sCT can be well characterized with a two-compartmental model after i.v. injection. However, significant differences in the compartmental transfer parameters (k12 and k21) in respect to [21] were obtained, noting that the stability of free sCT in serum in the current study was significantly higher. Free sCT quickly disappears from serum and the kinetics allow simple predictive modelling of its removal by degradation. From this, we further modelled release of sCT from conjugates, assuming a first order release mechanism. Simple equations allowed estimation of the parameter of physiological relevance in releasing sCT from sCT-P,(i.e. k_{rel}), and allowed comparison between the different MW conjugates. The decrease in k_{rel} in the presence of comb-shaped polymers of increasing MW was statistically significant and the data indicated that manipulation of MW within ranges that are acceptable from manufacturing, efficacy and toxicological standpoints will permit formulations that can extend the T½. A sensitivity of the release rate constant k_{rel} to differences in MW of the conjugated polymer of 0.053±0.016 ln (min^{-1}) reduction per kD was calculated. This parameter quantifies the effect of the conjugated polymer chain length on PK and provides indications on how to design appropriate conjugates for specific applications.

5. Conclusions

A PEG-based combed-shaped methacrylate polymer was conjugated to a specific amino acid of sCT to yield a pure bioactive conjugate, which retained receptor binding capacity. Conjugates of varying MW were made, purified and characterised using a simple economic process of living radical polymerisation. Relationships of MW with *in vitro* potency and efficacy were established. The largest conjugate (40 kDa) had an extended T½ upon i.v. injection to rats and this more than compensated for slight losses in potency and efficacy detected *in vitro*. Formulations of such conjugates may have potential for either long-acting systemic injection for osteoporosis or for local intra-articular delivery for treatment of osteoarthritis.

Acknowledgments

This study was funded by Science Foundation Ireland Strategic Research Cluster Grant 07/SRC/B1154.

References

[1] D.K. Malik, S. Baboota, A. Ahuja, S. Hasan, J. Ali, Recent advances in protein and peptide drug delivery systems. Current Drug Delivery 4 (2007) 141-151.
[2] J.H. Hamman, G.M. Enslin, A.F. Kotze, Oral delivery of peptide drugs: barriers and developments. BioDrugs 19 (2005) 165-177.
[3] S.M. Ryan, G. Mantovani, X. Wang, D.M. Haddleton, D.J. Brayden, Advances in PEGylation of important biotech molecules: delivery aspects. Expert Op. Drug Del. 5 (2008) 371-383.
[4] F.M. Veronese, G. Pasut, PEGylation, successful approach to drug delivery. Drug Discovery Today 10 (2005) 1451-1458.
[5] M. Hamidi, A. Azadi, P. Rafiei, Pharmacokinetic consequences of pegylation. Drug Delivery 13 (2006) 399-409.
[6] C. H. Chesnut 3rd, M. Azria, S. Silverman, M. Engelhardt, M. Olson, L. Mindeholm.

Salmon calcitonin: a review of current and future therapeutic indications. Osteoporosis. Int. 19 (2008) 479-491.
[7] B-C. Sondergaard, S. H. Madsen, T. Segovia-Silvestre, S. J. Paulsen, T. Christiansen, C. Pedersen, A-C. Bay-Jensen, M. A. Karsdal, Investigation of the direct effects of salmon calcitonin on human chondrocytes, BMC Musculoskeletal Disorders, 11 (2010) 62-71.
[8] M.A. Karsdal, K. Henriksen, M. Arnold, C. Christiansen, Calcitonin: a drug of the past or for the future? Physiologic inhibition of bone resorption while sustaining osteoclast numbers improves bone quality. BioDrugs 22 (2008) 137-144.
[9] H. Hoyer, G. Perera, A. Bernkop-Schnurch, Non-invasive delivery systems for peptides and proteins in osteoporosis therapy: a retro-perspective. Drug Dev. Ind. Pharm. (2009).
[10] M. A Karsdal, K. Henriksen, A. C. Bay-Jensen, B. Molloy, M. Arnold, , M. R. John, I. Byrjalsen, M. Azria, B. J. Riis, P. Qvist, C Christiansen, Lessons learned from the development of oral calcitonin: the first tablet formulation of a protein in Phase III clinical trials. J. Clin. Pharm. (2010). PMID: 20660294.
[11] S.M. Ryan, X. Wang, G. Mantovani, C.T. Sayers, D.M. Haddleton, D.J. Brayden, Conjugation of salmon calcitonin to a combed-shaped end functionalized poly(poly(ethylene glycol) methyl ether methacrylate) yields a bioactive stable conjugate. J. Control. Release 135 (2009) 51-59.
[12] P. Bailon, C.Y. Won, PEG-modified biopharmaceuticals. Expert Opin. Drug Deliv. 6 (2009) 1-16.
[13] F. Lecolley, L. Tao, G. Mantovani, I. Durkin, S. Lautru, D.M. Haddleton, A new approach to bioconjugates for proteins and peptides ("pegylation") utilising living radical polymerisation. Chem. Comm. 18 (2004) 2026-2027.
[14] L. Tao, G. Mantovani, F. Lecolley, D.M. Haddleton, Alpha-aldehyde terminally functional methacrylic polymers from living radical polymerization: application in protein conjugation "pegylation". J. Am. Chem. Soc. 126 (2004) 13220-13221.
[15] B. Le Droumaguet, J. Nicolas, Recent advances in the design of bioconjugates from controlled / living radical polymerization. Polymer Chemistry 1 (2010) 563-598.
[16] K.C. Lee, S.C. Moon, M.O. Park, J.T. Lee, D.H. Na, S.D. Yoo, H.S. Lee, P.P. DeLuca, Isolation, characterization, and stability of positional isomers of mono-PEGylated salmon calcitonins. Pharm. Res. 16 (1999) 813-818.
[17] S.B. Fowler, S. Poon, R. Muff, F. Chiti, C.M. Dobson, J. Zurdo, Rational design of aggregation-resistant bioactive peptides: reengineering human calcitonin. PNAS (USA) 102 (2005) 10105-10110.
[18] R.D.C. Team, *R*: *A language and environment for statistical computing*, R Foundation for Statistical Computing, Vienna, Austria. http://www.r-project.org. (2008) Accessed September, 2010.
[19] I. Hubatsch, E. G. Ragnarsson, P. Artursson, Determination of drug permeability and prediction of drug absorption in Caco-2 monolayers.Nat. Protoc. 2 (2007) 2111-2119.
[20] D.M. Bates, D.G. Watts, Non-linear regression analysis and its applications, Wiley, New York, (1988).
[21] M. Miyazaki, S. Nakade, K. Iwanaga, K. Morimoto, M. Kakemi, Estimation of bioavailability of salmon calcitonin from the hypocalcemic effect in rats (I):

pharmacokinetic-pharmacodynamic modeling based on the endogenous Ca regulatory system. Drug Metabolism and Pharmacokinetics 18 (2003) 350-357.
[22] C.W. Tornoe, H. Agerso, E.N. Jonsson, H. Madsen, H.A. Nielsen, Non-linear mixed-effects pharmacokinetic/pharmacodynamic modelling in NLME using differential equations. Computer Methods and Programs in Biomedicine 76 (2004) 31-40.
[23] C.W. Tornoe, H. Agerso, H.A. Nielsen, H. Madsen, E.N. Jonsson, Pharmacokinetic/pharmacodynamic modelling of GnRH antagonist degarelix: a comparison of the non-linear mixed-effects programs NONMEM and NLME. J. Pharmacokinetics Pharmacodynamics 31(2004) 441-461.
[24] J. C. Pinheiro, D. M. Bates, Mixed effects models in S and S-Plus. Springer (New York), 2002.
[25] A. C. Hindmarsh, ODEPACK, A Systematized Collection of ODE Solvers, In: Scientific Computing, R. S. Stepleman et al. (Eds.), North-Holland,Amsterdam, (1983) (Vol. 1 of IMACS Transactions on Scientific Computation),pp. 55-64.
[26] M. J. Lindstrom, D. M. Bates, Non-linear mixed effects models for repeated measures data, Biometrics 46 (1990), 673-687.
[27] C. T. Sayers, G. Mantovani, S. M. Ryan, R. K. Randev, O. Keiper, O. I. Leszczyszyn,, C. Blindauer, D. J. Brayden, D. M. Haddleton (2009), Site-specific N-terminus conjugation of poly($mPEG_{1100}$) methacrylates to salmon calcitonin: synthesis and preliminary biological evaluation, Soft Matter 5 (2009) 3038-3046.
[28] C. T. Sayers. Conjugation of peptides with polymers synthesised via living radical polymerisation. Ph.D. Thesis (2008) University of Warwick, UK.
[29] S. Jevsevar, M. Kunstelj, V.G. Porekar, PEGylation of therapeutic proteins. Biotechnol. J. 5 (2010) 113-128.
[30] C. J. Fee, Size comparison between proteins PEGylated with branched and linear poly(ethylene glycol) molecules. Biotechnol. Bioeng. (2007) 725-731.
[31] A. Bendele, J. Seely, C. Richey, G. Sennello, G, Shopp, Short communication: renal tubular vacuolation in animals treated with polyethylene-glycol-conjugated proteins. Toxicol. Sci. 42 (1998)152-157.
[32]. S. Walsh, A. Steward, D. M. Haddleton, R. Palmer. Renal epithelial cell vacuolisation induced by cumulative doses of PEG, but not PolyPEG®. PEGS 2008, Boston, MA.
http://www.warwickeffectpolymers.co.uk/docs/PolyPEGAbsenceofVacuolisationPosterPEGS2008.pdf. Accessed May, 2010.
[33] P. Bailon, A. Palleroni, C.A. Schaffer, C.L. Spence, W.J. Fung, J.E. Porter, G.K. Ehrlich, W. Pan, Z.X. Xu, M.W. Modi, A. Farid, W. Berthold, M. Graves, Rational design of a potent, long-lasting form of interferon: a 40 kDa branched polyethylene glycol-conjugated interferon alpha-2a for the treatment of hepatitis C. Bioconjug. Chem. 12 (2001) 195-202.
[34] Y.S. Youn, J.Y. Jung, S.H. Oh, S.D. Yoo, K.C. Lee, Improved intestinal delivery of salmon calcitonin by Lys18-amine specific PEGylation: stability, permeability, pharmacokinetic behavior and in vivo hypocalcemic efficacy. J. Control. Release 114 (2006) 334-342.
[35] K.C. Lee, K.K. Tak, M.O. Park, J.T. Lee, B.H. Woo, S.D. Yoo, H.S. Lee, P.P. DeLuca, Preparation and characterization of polyethylene-glycol-modified salmon calcitonins. Pharm. Dev. and Tech. 4 (1999) 269-275.

[36]. Y.S. Youn, M.J. Kwon, D.H. Na, S.Y. Chae, S. Lee, K.C. Lee, Improved intrapulmonary delivery of site-specific PEGylated salmon calcitonin: optimization by PEG size selection. J. Control. Release 125 (2008) 68-75.
[37] Y.S. Youn, D.H. Na, K.C. Lee, High-yield production of biologically active mono-PEGylated salmon calcitonin by site-specific PEGylation. J. Control. Release 117 (2007) 371-379.
[38] T. Buclin, J.P. Randin, A.F. Jacquet, M. Azria, M. Attinger, F. Gomez, P. Burckhardt, The effect of rectal and nasal administration of salmon calcitonin in normal subjects. Calcified Tissue Internat. 41 (1987) 252-258.
[39] Y.W. Jo, Y.S. Youn, S.H. Lee, B.M. Kim, S.H. Kang, M. Yoo, E.C. Choi, K.C. Lee, Long-acting interferon-α 2a modified with a trimer-structured polyethylene glycol: preparation, in vitro bioactivity, in vivo stability and pharmacokinetics. Int J. Pharm. 309 (2006) 87-93.
[40] S.V. Komarova, R.J. Smith, S.J. Dixon, S.M. Sims, L.M. Wahl, Mathematical model predicts a critical role for osteoclast autocrine regulation in the control of bone remodeling. Bone 33 (2003) 206-215.